Astro2020 Science White Paper

Star Formation in Different Environments: The Initial Mass Function

Thematic Areas: ☐ Planetary Systems ☑ Star and Planet Formation
☐ Formation and Evolution of Compact Objects ☐ Cosmology and Fundamental Physics
☐ Stars and Stellar Evolution ☑ Resolved Stellar Populations and their Environments
☐ Galaxy Evolution ☐ Multi-Messenger Astronomy and Astrophysics

Principal Author:
Name: Matthew Hosek Jr.
Institution: University of California at Los Angeles
Email: mwhosek@astro.ucla.edu

Co-authors: (names and institutions)
Jessica R. Lu (University of California at Berkeley)
Morten Andersen (Gemini Observatory)
Tuan Do (University of California at Los Angeles)
Dongwon Kim (University of California at Berkeley)
Nicholas Z. Rui (University of California at Berkeley)
Peter Boyle (University of California at Berkeley)
Benjamin F. Williams (University of Washington)
Sukanya Chakrabarti (Rochester Institute of Technology)
Rachael L. Beaton (Princeton University)

Abstract:

The stellar initial mass function (IMF) is a fundamental property of star formation, offering key insight into the physics driving the process as well as informing our understanding of stellar populations, their by-products, and their impact on the surrounding medium. While the IMF appears to be fairly uniform in the Milky Way disk, it is not yet known how the IMF might behave across a wide range of environments, such as those with extreme gas temperatures and densities, high pressures, and low metallicities. We discuss new opportunities for measuring the IMF in such environments in the coming decade with JWST, WFIRST, and thirty-meter class telescopes. For the first time, we will be able to measure the high-mass slope and peak of the IMF via direct star counts for massive star clusters across the Milky Way and Local Group, providing stringent constraints for star formation theory and laying the groundwork for understanding distant and unresolved stellar systems.

Introduction

Star formation has played a critical role in shaping the Universe we observe today. A fundamental property of star formation is the Initial Mass Function (IMF), which describes the distribution of stellar masses created in a star-forming event. The IMF provides key insights into the underlying physics driving star formation (e.g. Krumholz, 2014; Offner et al., 2014), and is a vital ingredient in many areas of astrophysics, such as star formation over cosmic time (e.g. Narayanan & Davé, 2012; Ferré-Mateu et al., 2013), the mass assembly and evolution of galaxies (e.g. Clauwens et al., 2016; Gutcke & Springel, 2019), compact object production and merger rates (e.g. Banerjee, 2017; Mapelli & Giacobbo, 2018), and stellar feedback (e.g. Dale, 2015).

Despite its importance, we still lack a model of star formation that predicts the IMF of a stellar population produced by a given molecular cloud. Observations suggest that the IMF is fairly uniform within the Milky Way disk and local solar neighborhood (Bastian et al., 2010, for review). However, these populations span a limited range of environmental conditions. There is now evidence that the IMF varies in more extreme environments such as in the Galactic Center (e.g. Lu et al., 2013), the most massive elliptical galaxies (e.g. van Dokkum & Conroy, 2010), or the least luminous Milky Way satellites (e.g. Geha et al., 2013). These claims of a non-standard IMF are debated and the underlying astronomical measurements cannot easily be improved upon with current space-based and ground-based observatories.

We discuss new opportunities for investigating the IMF across a wide range of environments in the coming decade. *With advanced observing facilities such as the James Webb Space Telescope (JWST), Wide-Field Infrared Survey Telescope (WFIRST), and 30m class telescopes, we can precisely measure the IMF down to $\leq 0.2\ M_\odot$ via star counts for star clusters across the Milky Way and Local Group.* For the first time, we will be able to directly measure both the high-mass slope and peak mass of the IMF for these populations and characterize how they vary with environment. This allows us to distinguish between different physical processes that influence star formation and inform how we should interpret observations of unresolved stellar systems.

Current Status: IMF Variations with Environment?

The quest for a predictive theory of star formation as a function of initial conditions (metallicity, density, external pressure) is far from over. Most observations reveal a "universal" IMF, and, not surprisingly, many diverse models are able to "explain" it. Under intense scrutiny, most claims of detecting a non-universal IMF wither (e.g. Bastian et al., 2010; Luhman, 2018), though there are some unexplained surprises. Some of the most persistent claims are from IMF measurements via indirect techniques (population synthesis, dynamics, and strong lensing) toward giant elliptical galaxies (e.g. van Dokkum & Conroy, 2010; Treu et al., 2010; Conroy & van Dokkum, 2012; Cappellari et al., 2012; La Barbera et al., 2013; Spiniello et al., 2014; Martín-Navarro et al., 2015; Conroy et al., 2017; van Dokkum et al., 2017; La Barbera et al., 2017; Parikh et al., 2018). These studies suggest that the IMF becomes increasingly bottom-heavy (i.e., an overabundance of low-mass stars) with increasing galaxy velocity dispersion and/or α-element enhancement. However, concerns have been raised about the impact of systematics on these analyses, such as elemental abundance gradients (e.g. McConnell et al., 2016; Zieleniewski et al., 2017) or galaxy mass modeling (e.g. Leier et al., 2016). In addition, the internal consistency of IMF determinations using these indirect methods has yet to be established (e.g. Newman et al., 2017).
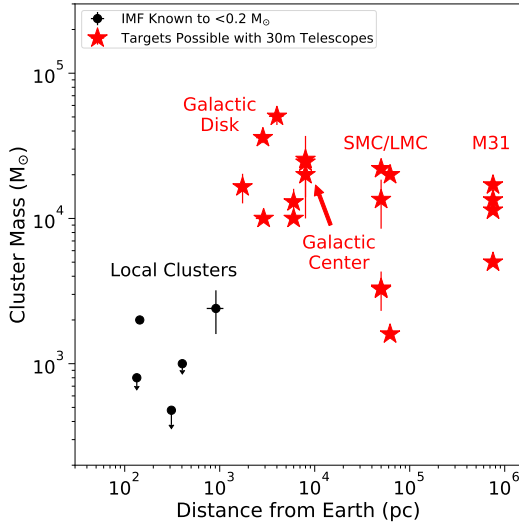
Figure 1 Examples of young and massive clusters for which we can measure the IMF to $\leq$ 0.2 M$_\odot$ with 30m class telescopes (red stars) compared to local star forming regions where this measurement has already been made (black points). The substantial gain in both spatial resolution and sensitivity allows us to probe a wide range of environments for the first time.
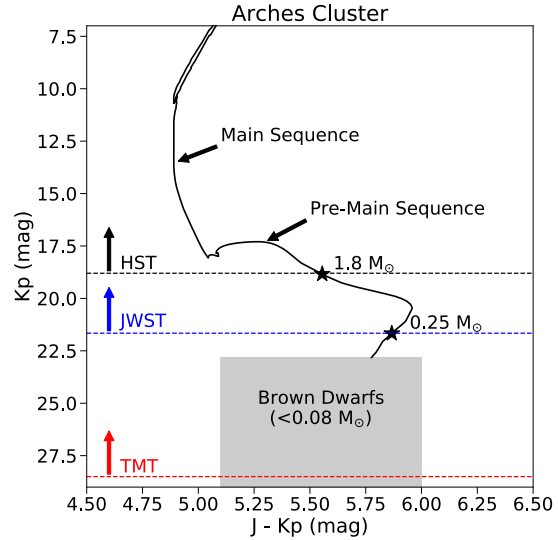
Figure 2 The TMT confusion limit (red dotted line) compared to the JWST confusion limit (blue dotted line) and HST completeness limit (black dotted line) for the Arches cluster, a $\sim$3 Myr old cluster near the Galactic Center. With 30m class telescopes, we can resolve objects well into the brown dwarf regime.

On the other hand, direct star counts have found top-heavy IMFs (i.e. an overabundance of high-mass stars) for two massive clusters at the Galactic Center (Lu et al., 2013; Hosek et al., 2019) and the 30 Dorodus starburst region in the LMC (Schneider et al., 2018). These clusters are thought to form in significantly different conditions than typical clusters in the Milky Way disk; for example, the Galactic Center has been shown to exhibit similar gas densities, temperatures, and kinematics as starburst galaxies (Kruijssen & Longmore, 2013; Ginsburg et al., 2016). On the other end of the spectrum, some ultra-faint dwarf galaxies have also been reported with top-heavy IMFs, perhaps due to the low metallicity or overall stellar mass of these systems (Geha et al., 2013; Gennaro et al., 2018a), though others seem more consistent with the Milky Way disk (Gennaro et al., 2018b). Such direct measurements of the IMF face challenges as well, including sample contamination, stellar multiplicity, and limited stellar mass ranges. Unfortunately, nearby and better-studied star forming regions are poor analogues for the diverse star forming events at extreme temperatures, densities, pressures and low metallicities which may characterize environments in the early Universe, galactic nuclei, and merger events.

The Next Step: Direct IMF Measurements Across Different Environments

JWST, WFIRST, and 30m telescopes provide the ability to directly measure the IMF down to $\leq$0.2 M$_\odot$ across a range of environments in the Milky Way and Local Group. Of particular interest are young (<150 Myr) and massive (> 10^3 M$_\odot$) clusters, which exhibit a single-age stellar population with a well-sampled IMF across a large mass range. Available targets include clusters in the disk and center of the Milky Way (e.g. Arches cluster, Westerlund 1), the LMC and
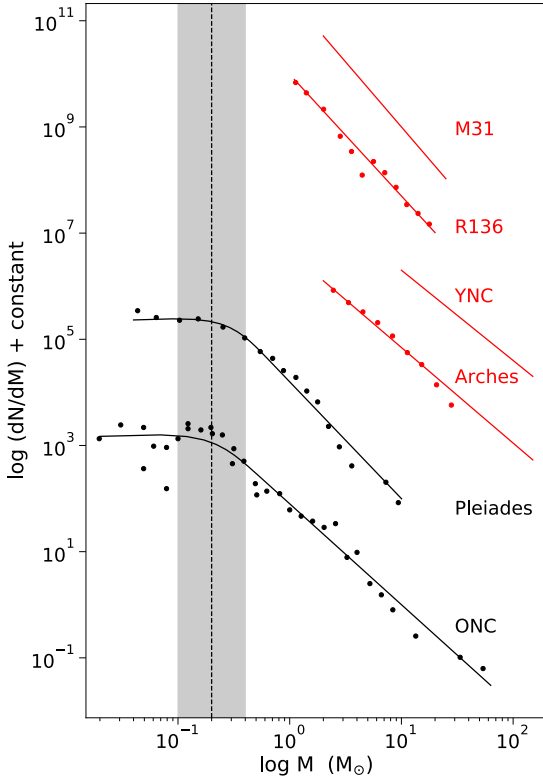
3

Figure 3 Current IMF measurements for selected local star forming regions (black) and interesting future objects (red). With 30m class telescopes, we will be able to directly measure the IMF down to the peak mass (black shaded region) and beyond, characterizing its behavior across a wide range of environments. References: ONC (Slesnick et al., 2004; De Marchi et al., 2010), Pleiades (Moraux et al., 2003; De Marchi et al., 2010), Arches (Hosek et al., 2019), YNC (Lu et al., 2013), R136 (Andersen et al., 2009), and M31 young clusters (Weisz et al., 2015).

SMC (e.g. R136, NGC 602), and M31 (e.g. KW258). While the IMF has been measured to such depths in local star forming regions, these targets are significantly more massive and span a wide range of conditions including the Galactic Center, low metallicities, and starburst-like environments (Figure 1). These are highly crowded clusters and the lowest-mass stars are very faint, and so high spatial resolution and sensitivity are essential in order to make this measurement (Table 1). For example, current resolved imaging studies of clusters at the Galactic Center are limited to the high-mass stars ($M > 2\,M_\odot$), at best. With 30m telescopes, the confusion limit is not reached until beyond the hydrogen-burning limit (Figure 2)! Wide-field observations by JWST and WFIRST allows for efficient coverage of the lower-density outer regions of Milky Way clusters which subtend $\gtrsim 1'$ on the sky.

Critically, achieving a depth of $\leq 0.2\,M_\odot$ allows us to accurately measure the peak of the IMF as well as the high-mass slope, as has been achieved for local star forming regions (Figure 3). For a typical $10^4\,M_\odot$ cluster, simulations by El-Badry et al. (2017) show that this depth is required to distinguish between the proposed lognormal (e.g. Chabrier, 2003) and broken power-law (e.g. Kroupa et al., 2013) forms of the IMF, an uncertainty that hinders IMF measurements at low stellar masses today. In addition, assuming a log-normal IMF, they find that when observations reach $0.2\,M_\odot$ the degeneracy between the characteristic mass (i.e. peak mass) and width is broken and strong constraints can be placed on both parameters. The peak of the IMF is a key constraint for star formation models since it is not a scale-free parameter (unlike the high-mass slope) and thus additional physics beyond gravity-driven accretion or turbulence is required to set it (Krumholz, 2014). Possibilities include the thermal Jeans Mass (e.g. Larson, 2005), the turbulent Jeans Mass (e.g. Hennebelle & Chabrier, 2008), and radiative feedback (e.g. Bate, 2009). Predictions for how the IMF, and in particular the peak mass of the IMF, behaves in different

Table 1.   Properties of Young Clusters in Different Environments

Cluster	Mass	Distance	Angular Diameter	Proper Motion for 10 km s^{-1}	0.2 M$_\odot$ Mag
	(M$_\odot$)	(kpc)	(arcsec)	(mas yr^{-1})	(K mag)
Orion	$\sim 10^3$	0.4	516	5.28	12.0
Wd1	5x10^4	4.0	360	0.53	18.9
Arches	2.5x10^4	8.0	150	0.26	21.9
R136	2.2x10^4	50	38.6	0.04	23.0
KW258	1.1x10^4	753	2.45	3x10^{-3}	28.9

environments changes depending on which of these processes dominate. Thus, exploring these environments is a valuable tool for understanding star formation.

Methodology

A common method to directly measure the IMF is to obtain the fluxes from the resolved stars, construct a color-magnitude diagram or luminosity function (correcting for differential reddening, if necessary), and then compare the population to theoretical isochrones from stellar evolution models. Due to their youth, the clusters are still partly embedded in the molecular cloud out of which they formed these studies are easiest performed in the NIR. Purely photometric studies of young clusters are often limited by field contamination, as differential extinction makes it difficult to identify cluster members via photometry alone. In addition, the fraction of field stars increases at fainter magnitudes, as the cluster luminosity function eventually turns over but the field star luminosity function continues to increase. This issue can be mitigated by using proper motions in addition to photometry to isolate cluster members, as has been demonstrated for the Arches cluster (Figure 4, Hosek et al., 2019).

IMF measurements can further be refined by measuring stellar temperatures from NIR spectra and constructing an HR diagram, which helps constrain the mass-luminosity relationship. In addition, spectroscopy of a subset of cluster candidates can be used to quantify and correct for field contamination that remains after membership selection. Spectral analysis can be performed using comparisons to both model spectra (e.g. Repolust et al., 2005) and reference spectra from nearby star forming regions (e.g. Luhman et al., 2016). These measurements at high stellar densities and large distance requires sensitive integral-field or multi-object spectrographs with R $\gtrsim$ 4000.

The IMF observations will produce cluster star catalogs containing photometry, proper motions, stellar masses, and membership probabilities for the resolved stars, as well as some spectroscopic measurements. A large amount of ancillary science can be achieved with such data, including: 1) star cluster evolution and dynamics, taking advantage of the age spread across the clusters; 2) stellar evolution, as the high-quality cluster samples over a wide mass range at different ages and metallicities are a strong observational test for stellar evolution and atmosphere models; and 3) circumstellar disk evolution as a function of stellar mass, metallicity, and cluster environment. In addition, the clusters discussed here further serve as references themselves; objects such as 30
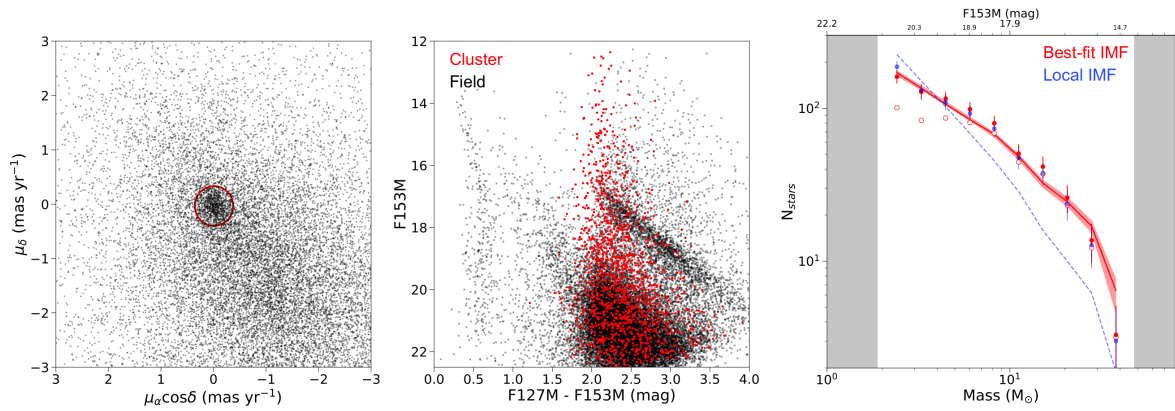
Figure 4 **Left:** A proper motion diagram of the Arches cluster. Stars bound to the cluster have similar proper motions and thus form a well-defined clump (red circle), from which cluster membership can be determined. **Middle:** The *HST* color-magnitude diagram of the Arches cluster field, with cluster member candidates highlighted in red. The overlap between the cluster and field populations causes significant contamination without proper-motion selection. **Right:** The Arches IMF (observations as red points, best-fit model as red shaded region) measured to down to 1.8 M$_\odot$ from Hosek et al. (2019). The cluster is found to have an overabundance of high-mass stars relative to nearby star forming regions (blue dotted line).

Doradus and its central cluster R136 are used as templates for the high-z unresolved star clusters where their properties have to be determined from their integrated properties.

Recommendations

A **thirty-meter diameter optical/NIR telescope equipped with adaptive optics** is the primary recommendation to advance observational studies of the stellar initial mass function over a wide range of environments. In particular:

- The adaptive optics system should provide wide field-of-view imaging capabilities with uniform correction in order to maximize effective observing area

- The point-spread function will need to be known to high accuracy over the field, in order to take advantage of the huge gains provided by astrometry and proper motions

- Moderate resolution (R $\sim$ 4000) spectroscopy from an integral field or multi-object infrared spectrograph, also supported by an adaptive optics system, is valuable to constrain the mass-luminosity relationship and quantify field contaminants

- Having facilities in both hemispheres is required to take full advantage of available targets

Such a facility has **strong synergy with upcoming space telescopes such as JWST and WFIRST**. The large field of view provided by the space telescopes can efficiently observe the lower-density outer regions of a cluster, while the 30m telescopes can focus on the innermost crowded regions. Together, these observations ensure full spatial coverage of the target cluster.

References

Andersen, M., Zinnecker, H., Moneti, A., et al. 2009, ApJ, 707, 1347

Banerjee, S. 2017, MNRAS, 467, 524

Bastian, N., Covey, K. R., & Meyer, M. R. 2010, ARA&A, 48, 339

Bate, M. R. 2009, MNRAS, 392, 1363

Cappellari, M., McDermid, R. M., Alatalo, K., et al. 2012, Nature, 484, 485

Chabrier, G. 2003, PASP, 115, 763

Clauwens, B., Schaye, J., & Franx, M. 2016, MNRAS, 462, 2832

Conroy, C., & van Dokkum, P. G. 2012, ApJ, 760, 71

Conroy, C., van Dokkum, P. G., & Villaume, A. 2017, ApJ, 837, 166

Dale, J. E. 2015, New A Rev., 68, 1

De Marchi, G., Paresce, F., & Portegies Zwart, S. 2010, ApJ, 718, 105

El-Badry, K., Weisz, D. R., & Quataert, E. 2017, MNRAS, 468, 319

Ferré-Mateu, A., Vazdekis, A., & de la Rosa, I. G. 2013, MNRAS, 431, 440

Geha, M., Brown, T. M., Tumlinson, J., et al. 2013, ApJ, 771, 29

Gennaro, M., Tchernyshyov, K., Brown, T. M., et al. 2018a, ApJ, 855, 20

Gennaro, M., Geha, M., Tchernyshyov, K., et al. 2018b, ApJ, 863, 38

Ginsburg, A., Henkel, C., Ao, Y., et al. 2016, A&A, 586, A50

Gutcke, T. A., & Springel, V. 2019, MNRAS, 482, 118

Hennebelle, P., & Chabrier, G. 2008, ApJ, 684, 395

Hosek, Jr., M. W., Lu, J. R., Anderson, J., et al. 2019, ApJ, 870, 44

Johnson, L. C., Seth, A. C., Dalcanton, J. J., et al. 2015, ApJ, 802, 127

Kroupa, P., Weidner, C., Pflamm-Altenburg, J., et al. 2013, The Stellar and Sub-Stellar Initial
    Mass Function of Simple and Composite Populations, ed. T. D. Oswalt & G. Gilmore, 115

Kruijssen, J. M. D., & Longmore, S. N. 2013, MNRAS, 435, 2598

Krumholz, M. R. 2014, Phys. Rep., 539, 49

La Barbera, F., Ferreras, I., Vazdekis, A., et al. 2013, MNRAS, 433, 3017

La Barbera, F., Vazdekis, A., Ferreras, I., et al. 2017, MNRAS, 464, 3597

Larson, R. B. 2005, MNRAS, 359, 211

Leier, D., Ferreras, I., Saha, P., et al. 2016, MNRAS, 459, 3677

Lu, J. R., Do, T., Ghez, A. M., et al. 2013, ApJ, 764, 155

Luhman, K. L. 2018, AJ, 156, 271

Luhman, K. L., Esplin, T. L., & Loutrel, N. P. 2016, ApJ, 827, 52

Mapelli, M., & Giacobbo, N. 2018, MNRAS, 479, 4391

Martín-Navarro, I., Barbera, F. L., Vazdekis, A., Falcón-Barroso, J., & Ferreras, I. 2015, MNRAS, 447, 1033

McConnell, N. J., Lu, J. R., & Mann, A. W. 2016, ApJ, 821, 39

Moraux, E., Bouvier, J., Stauffer, J. R., & Cuillandre, J.-C. 2003, A&A, 400, 891

Narayanan, D., & Davé, R. 2012, MNRAS, 423, 3601

Newman, A. B., Smith, R. J., Conroy, C., Villaume, A., & van Dokkum, P. 2017, ApJ, 845, 157

Offner, S. S. R., Clark, P. C., Hennebelle, P., et al. 2014, Protostars and Planets VI, 53

Parikh, T., Thomas, D., Maraston, C., et al. 2018, MNRAS, 477, 3954

Repolust, T., Puls, J., Hanson, M. M., Kudritzki, R.-P., & Mokiem, M. R. 2005, A&A, 440, 261

Schneider, F. R. N., Sana, H., Evans, C. J., et al. 2018, Science, 359, 69

Slesnick, C. L., Hillenbrand, L. A., & Carpenter, J. M. 2004, ApJ, 610, 1045

Spiniello, C., Trager, S., Koopmans, L. V. E., & Conroy, C. 2014, MNRAS, 438, 1483

Treu, T., Auger, M. W., Koopmans, L. V. E., et al. 2010, ApJ, 709, 1195

van Dokkum, P., Conroy, C., Villaume, A., Brodie, J., & Romanowsky, A. J. 2017, ApJ, 841, 68

van Dokkum, P. G., & Conroy, C. 2010, Nature, 468, 940

Weisz, D. R., Dolphin, A. E., Skillman, E. D., et al. 2015, ApJ, 804, 136

Zieleniewski, S., Houghton, R. C. W., Thatte, N., Davies, R. L., & Vaughan, S. P. 2017, MNRAS, 465, 192